-RESEARCH PAPER-

International Journal of Mining and Geo-Engineering

IJMGE

IJMGE 60-2 (2026) 149-159

DOI:10.22059/IJMGE.2026.401926.595303

High-grade zone estimation using the SVM and BPPN algorithms in Chah Firuzeh porphyry copper deposit

Kamran Mostafaei [a, *], Ardeshir Hezarkhani [b], Shahoo Maleki [b], Mohammad Zamani Ahmad Mahmoudi [c], Mitra Khalilidermani [c] and Dariusz Knez [c]

[a] *Department of Mining Engineering, Faculty of Engineering, University of Kurdistan, Sanandaj, Iran.*

[b] *Faculty of Mining Engineering, Amirkabir University of Technology, Tehran, Iran.*

[c] *Department of Drilling and Geo-engineering, Faculty of Drilling, Oil and Gas, AGH University of Krakow, Krakow, Poland.*

Article History:

Received: 06 September 2025.

Revised: 18 November 2025.

Accepted: 05 May 2026.

ABSTRACT

In the Chah Firuzeh porphyry copper deposit, a number of thirteen coring boreholes were drilled to evaluate the copper grades in the anomaly. While twelve of the boreholes intersected only the low- and medium-grade copper zones, the borehole CHF06 reached a high-grade zone. As such a high-grade zone is economically invaluable in the financial perspective of the mine, the corresponding copper grades must be estimated precisely. The primary goal of the current study is to estimate the copper grades in such high-profit zone using three artificial intelligence (AI) techniques: Support Vector Machine (SVM) and Back Propagation Neural Network (BPNN). Due to the porphyry nature of deposit, no clear relation was found between the copper grades of the borehole CHF06 and the rest. To address this issue, the Genetic Algorithm-Artificial Neural Network (GA-ANN) and Principal Component Analysis (PCA) algorithms were utilized to choose the best input dataset for those three AI techniques. Both the GA-ANN and PCA algorithms detected that the copper grades of the boreholes CHF05, CHF21, CHF24, and CHF26 are the most appropriate input data to be imported into the SVM and BPNN models. After grade estimation, the R-square (R^2) of the SVM and BPNN, techniques were obtained as 0.98 and 0.72, respectively. Moreover, further analysis uncovered that the SVM model has the least sensitivity to the ratio of training data to testing data. Hence, the SVM approach was recognized as the most reliable AI technique to accurately solve the complex resource estimation problems in mining projects. This key finding implies that a SVM estimator can be applied not only for the uniform-mineralization ores but also for the deposits exhibiting a highly inconsistent grade-trend in their structures.

Keywords: *Grade estimation, Chah Firuzeh copper deposit, SVM, BPNN, GA-ANN, PCA.*

1. Introduction

The main objective of the exploratory drilling operations is to create a 3D geological model that contains the grade and volume of the different minerals in the deposit. During a drilling operation, usually tens of boreholes are drilled, and simultaneously, thousands of rock coring samples are taken from the subsurface formations. Then, the coring samples are transferred to the specific laboratories, and the percentage of potential economic minerals, e.g. copper, gold, silver, iron, etc., in each rock sample is measured. If one mineral has a grade larger than the national (or international) cut-off grade (the least grade which is profitable for the mining project), a feasibility study is conducted to evaluate the profitability of the mineral exploitation. The cornerstone of such a feasibility study is called "resource estimation" in which the grade and total volume of the valuable mineral are calculated [1]. After resource estimation, and importing of the mineral price (which is proportional to the mineral grade), one can compute the total economic value of the resource. As a result, the 3D geological model is turned into an "economic block model" that contains thousands of rock blocks so that each block has an average grade, volume, and economic value. Thus, an accurate estimation of the mineral grade will affect the economic value of the total resource, and more importantly, it contributes to starting (or leaving) the decision of the mining operation in an intact deposit.

The accuracy of a resource estimation task is commonly affected by several factors, such as inadequate exploratory boreholes, problematic mineralization type (porphyry, vein, etc.), potential anisotropies in the mineral distribution, and last but not least the grade estimation technique. Regarding the latter case, geostatistical and AI techniques are commonly utilized to estimate mineral grades in explored deposits [2,3]. A geostatistical method, e.g. the ordinary kriging (OK), functions through the assumption of the stationary conditions. In addition, it is a linear model established on the local neighborhood structure.

Oppositely, AI techniques, e.g. SVM and BPNN, are considered as the non-linear model-free estimators, which are markedly robust, even in the presence of a highly noisy input data. In fact, some AI techniques deliver a better grade estimation especially when there are non-linear spatial trends in the input data. It is noteworthy that such conditions may violate the stationary assumption of the OK estimator.

For instance, it is widely accepted that the porphyry copper-gold and

* Corresponding author. *E-mail address:* : k.mostafaei@uok.ac.ir (K. Mostafaei).

copper-molybdenum deposits exhibit nonlinear behaviors. Therefore, for such porphyry deposits, application of a powerful nonlinear estimator to estimate the grades of the copper, molybdenum, and gold is extremely much-needed.

Artificial Neural Network (ANN) techniques are considered as the potent tools to solve the highly complicated problems. Regarding the resource estimation of mining projects, several researchers have used such techniques [4-14]. The ANN techniques require a series of the input and output data to reveal the hidden correlations between the different variables [15]. Generally, the input data includes the grades of the economic minerals obtained from the rock coring samples in the field [16]. Similarly, the output data contains the grades of the valuable minerals in the different spots of the deposit (note that such output data is then used for creation of the economic block model). The majority of the ANN techniques carry out the estimation process using a function approximation [17-19]. Hence, such ANN techniques may cause a very poor generalization [20], or even over-fitting, if the variables incorporated in the modeling process are not properly selected.

The SVM technique deploys the support vector regression (SVR) for regression problems. It is a powerful machine learning (ML) approach established by Vapnik in the 1990s [21]. In the domain of resource estimation, the SVM approach has been frequently adopted for iron deposits [22]. The SVR algorithm utilizes statistical learning theory to generate the hidden parameters. In the solution of complex problems, the SVM approach exhibits a superior performance mainly due to its' significant generalization ability against the potential noise and interference within the input data [22]. On a positive note, the SVM approach is very efficient in solving the problems with the least number of the input data [23, 22]. It can be expressed that the major advantages of the SVM approach stem from three sources: firstly, it is remarkably robust in learning (training) process, even if only a restricted number of training data are existent; secondly, it minimizes the estimation error so that a reasonable prediction is performed for output parameters; and thirdly, it is more computation-efficient, and time-efficient in contrast to other AI techniques [22]. So, the SVM technique have been used in mineral exploration research [24-29].

Recent advances in deep learning have created new opportunities for solving complex geoscientific problems, with architecture like LSTM networks showing particular promise in processing sequential geophysical data [30]. While these methods excel with large-scale datasets, our study employs SVM and BPNN approaches which offer proven effectiveness for mineral grade estimation with limited borehole data, ensuring robust performance while maintaining computational efficiency.

The principal innovation of this study lies in addressing a common yet challenging scenario in porphyry deposit exploration: estimating high-grade zones using exclusively low- and medium-grade data from other boreholes. While SVM and ANN are established methods, their novel application here involves an integrated workflow combining GA-ANN and PCA for robust input selection. This approach is specifically tailored to solve the complex problem of grade estimation when direct data from the target high-grade zone is limited to a single borehole, a frequent practical challenge in mineral resource evaluation

The current research strives to evaluate the applicability of the SVM and BPNN techniques in estimation of the copper grades in high-grade zones using the low and medium grade zones. The studied area is the Chah Firuzeh porphyry copper deposit located in Kerman province, Iran. The results achieved from the utilization of the SVM and BPNN models are contrasted to reveal the applicability and accuracy of those three techniques in resource estimation problems.

2. Materials and Methods

2.1. Study area and geological setting

The Chah Firuzeh porphyry copper deposit is situated within the broader tectonic framework of the Sanandaj-Sirjan Zone (SSZ), a major NW-Se trending metallogenic belt in Iran. The SSZ exhibits a complex and protracted history of mineralization, hosting diverse deposit types formed during multiple tectonic episodes. The Malayer-Esfahan metallogenic belt (MEMB) within SSZ contains numerous Certaceous sediment-hosted Zn-Pb deposits. Such as Irankuh and Emarat, which formed in extensional basins related to the subduction of the Neotethyan oceanic plate [31, 32]. In contrast, the Chah Firuzeh deposit represents a distinct, younger Tertiary magmatic-hydrothermal system, genetically linked to Eocene-Oligocene are magmatism in SSZ [33].

This research has been conducted in the Chah-Firuzeh porphyry copper deposit situated 35 km far from the Shahre-babak town in Kerman province, Iran. The main in situ formations vary from the diorite/ granodiorite masses to the quartz-monzonite rocks. Figure 1 depicts the map of the primary lithotectonic formations in Iran, and the location of the Chah Firuzeh copper deposit [33]. The area is dominantly hummocky together with the abundant low-altitude terrains in the eastern part. The geological set-up has originated from the volcano-plutonism (Eocene), and magmatism (Pyrenean Orogeny in Oligocene) phenomena. Furthermore, the mineralization origin has been ascribed to the fluids related to the Pyrenean magmatism, and also, to the intensifying factors that have been contemporaneous tectonic stresses. Figure 2 illustrates a close up pertinent to the distribution of the different geological formations in the Chah Firuzeh copper deposit [34]. It is noteworthy the large Sar-Cheshmeh copper mine lies in the vicinity of the Chah Firuzeh porphyry deposit. The Sar-Cheshmeh copper mine is the second largest copper deposit in the world.

In the area, the porphyry granodiorite rocks compose the hosting formations of the mineralization process. Furthermore, the mineralization towards the south of the area is slightly porphyritic. Based on the coring samples, the main subsurface alteration is potassic while it partially turns to phyllic at the surface around the borehole CHF06. In addition, the gangue chiefly consists of quartz, carbonate, and sericite minerals.

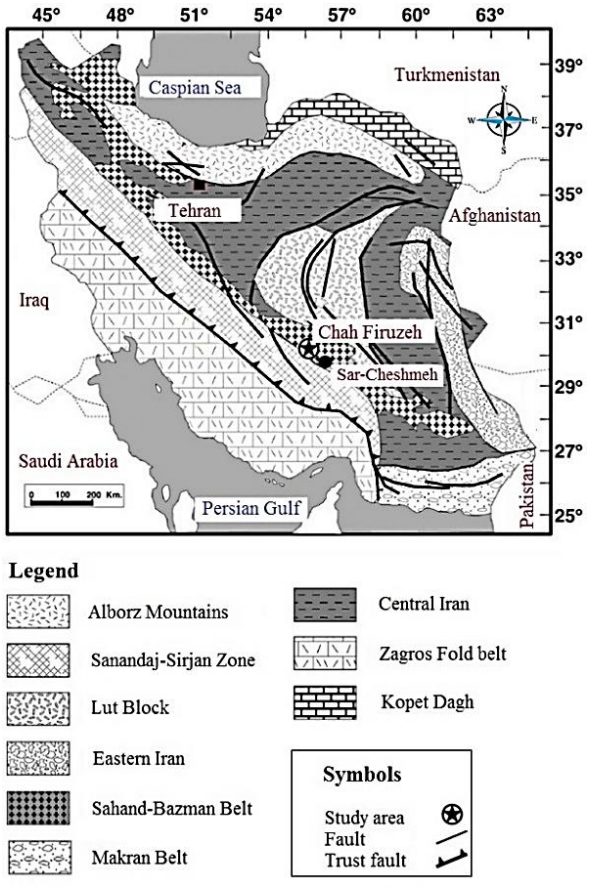

Figure. 1. Map of the primary lithotectonic formations in Iran, and the location of the Chah Firuzeh copper deposit [34].

Furthermore, the evidence of an abandoned mine is visible in the southern part. The conspicuous indicator is a tunnel with an inclination angle around 75°, and parallel to the North direction. It appears that the extracted ore mainly contained minerals such as malachite, azurite, and chrysocolla. In addition, scattered minerals such as pyrite and chalcopyrite crystals are observed in the siliceous veins and brecciated masses.

2.2. Dataset description

In this research, the raw input data contained the copper grades recorded from thirteen exploratory boreholes drilled in the Chah Firuzeh porphyry copper deposit. A number of twelve boreholes included the low-grade and medium-grade copper records; those boreholes were CHF01, CHF02, CHF05, CHF08, CHF09, CHF13, CHF20, CHF21, CHF22, CHF24, CHF25, and CHF26. On the other hand, only CHF06 delivered high-grade copper core samples. Figure 3 depicts the topography map together with the locations of the different boreholes in the area. The location of CHF06 borehole is illustrated in red.

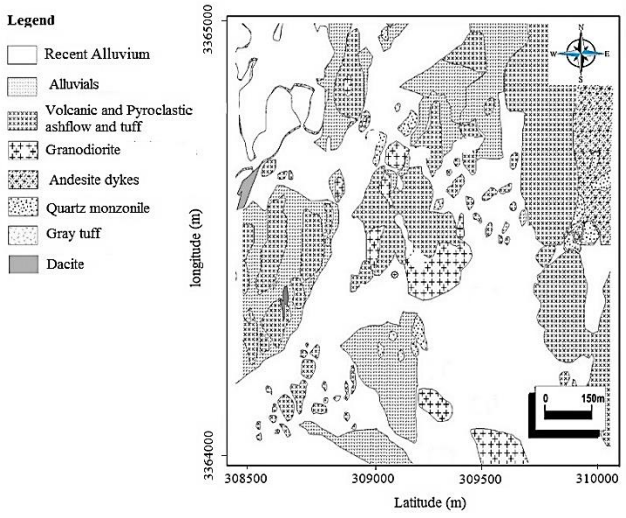

Figure 2. A close up related to the distribution of different geological formations in the Chah Firuzeh copper deposit [34].

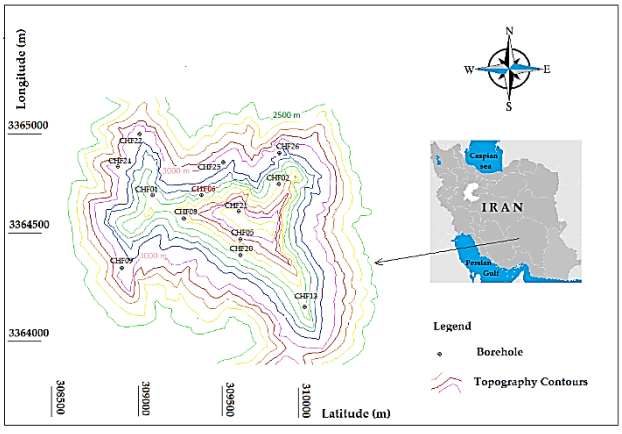

Figure 3. The topography map of the Chah Firuzeh copper deposit, and collars of the exploratory boreholes.

To correct the copper grades, the outliers along with the censored data were omitted for all thirteen boreholes. Each borehole had 169 copper grades (samples) which had been obtained in regular intervals of 1 m, from the depth of 170 to the depth of 350 m.

The thirteen boreholes used in this study, while limited in number, were strategically drilled based on preliminary geological and geophysical surveys to intercept the main mineralized zone. Their spatial distribution covers the key geological units and alteration patterns identified in the Chah Firuzeh deposit. Furthermore, the high density of sampling within each borehole (169 samples per borehole, totaling 2,197 samples) provides a robust dataset for machine learning applications. The primary objective was not to model the entire deposit, but to develop a methodology for estimating a specific high-grade zone using proximal data, for which this dataset is statistically adequate.

The recorded data were then divided into three categories: low-grade copper (0.15 ppm < Cu ≤0.30 ppm), medium-grade copper (0.30 ppm < Cu ≤0.50 ppm), and high-grade copper (0.50 ppm< Cu). In this research, firstly, the dataset related to the aforementioned twelve boreholes were used to train and test the SVM and BPNN models. To find the optimal number and combination of those boreholes, GA-ANN and PCA algorithms were adopted.

The solution process was carried out in the MATLAB program for implementation of the automated Bayesian regularization. Using such regularization markedly curtails the over fitting error. In MATLAB, the Neural Network Toolbox is not capable of handling the arbitrarily connected SVM and BPNN techniques. Due to this shortcoming, the codes were written and run without the utilization of MATLAB's Toolbox. At the first stage, a number of three data points in the vicinity were chosen. Then, those data points were deployed for the prediction step. Afterward, the normalization task of both input and output data was performed by Cox and Box technique.

2.3. Special framework and modeling

The spatial context of borehole data is fundamental to meaningful grade estimation in this study. To enable the machine learning models to capture both grade patterns and spatial relationships within the mineralization system, the three-dimensional coordinates (X, Y, Z) of each sample were explicitly incorporated as input features alongside copper grade values from selected boreholes.

While the primary focus of this research was to validate the predictive accuracy of SVM and BPNN models for estimating grade at specific target locations (notably the high CHF06 borehole), the methodology establishes a complete framework for full 3D resource modeling. For comprehensive spatial estimation, a regular 3D grid can be established within the mineralized zone volume, where the trained models would be applied to each grid node using its spatial coordinates and corresponding input data to predict copper values throughout the entire volume. This process effectively translates point-based predictions into a continuous 3D block model, demonstrating the scalability of the approach for complete resource estimation while maintaining the proof-of-concept validation scope of the current study.

2.4. SVM technique and implementation

As mentioned already, the SVR algorithm was utilized in regression problems; the SVR performs the learning process to find the function of $f(x)$ as an approximation of y with the least risk. Such a process is constituted upon the accessible autonomous and distributed data. The corresponding mathematic from can be stated through the following relationship [19, 22, 35],

$$(x_1, y_1), \ldots, (x_m, y_m) \subseteq (X \subseteq R^n \times Y \subseteq R) \quad (1)$$

The SVR algorithm deploys a limited number of the training data, which are known as Support Vectors (SVs), to compute the $f(x)$. Furthermore, in order to generate a sparseness attribute for the estimation process, the SVR applies an ε-sensitive loss function as [19, 22, 35],

$$|y - f(x)|_\varepsilon = \begin{cases} 0 & if \ |y - f(x)| \le \varepsilon \\ |y - f(x)| - \varepsilon & otherwise \end{cases} \quad (2)$$

In this relationship, $f(x)$ is the predicted function for the y, and the relevant error which is smaller than the ε boundary (ε tube), is not penalized (Figure 4).

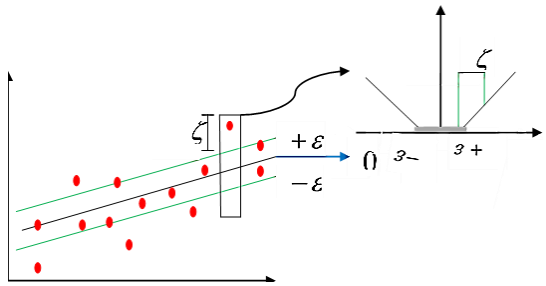

Figure 4. Diagram of the ε-insensitive loss function applied in the SVM algorithm [36].

In what follows, the SVR algorithm is described; if *f(x)* is a linear function of the variable of *x*, the pertinent mathematical form can be stated as the following formula [37].

$$f(x) = \langle w.x \rangle + b \; ; \; w, x \in X \subseteq R^n, b \in R \tag{3}$$

in this equation, *w* and *x* represent the *l*-dimensional weight vector and the *l*- dimensional feature space, respectively. Moreover, the parameter of *b* indicates the bias term. The symbol of $\langle . \rangle$ represents the inner product of two vectors in the Hilbert space. Through the ε-SVR, the *f(x)*, which delivers the output values, is estimated with acceptable deviations from the available training data [38]. In other words, the complexity of *f(x)* is restricted by the values of ε. Therefore, the low values of ε penalize a big percentage of the data, and consequently, it may give rise to creation of tight approximating models. Having said this, the higher values of ε cause less penalization of the training data, and consequently, they bring about loose approximating models. Due to this matter, it can be claimed that a close scrutiny must be conducted to select a proper value of ε for generalization of the regression models.

To determine the estimation function of *f(x)*, some AI techniques, e.g. ANNs, minimize the empirical risk function. However, in the SVM algorithm, it is more efficient to minimize the regulated risk function, R_{reg}, rather than the empirical one. R_{reg} is mathematically described in the underlying form [39, 36],

$$R_{reg}[f] = \frac{1}{2}||w||^2 + C.R^{\varepsilon}_{emp}[f] \; where \; R^{\varepsilon}_{emp}[f] = \frac{1}{m}\sum_{i=1}^{m} |y_i - f(x_i)|_{\varepsilon} \tag{4}$$

In this equation, R_{emp} and *C* represent the empirical error and the regularization coefficient, respectively. The latter reflects the complexity extent of the approximation function; it penalizes the error through minimizing both training error and the model complexity. As a matter of fact, minimization of R_{reg} is considered as the cornerstone of the structural risk minimization theory. This theory miniaturizes both training error and the model complexity to deliver the minimum potential risk. This key concept boosts the SVR generalization capability [40, 41].

If the previous equation is minimized, it will be the tantamount to the underlying convex constrained quadratic optimization problem [42].

$$L(w, \xi, \xi') = \frac{1}{2} \|w\|^2 + C \sum_{i=1}^{N} (\xi_i + \xi_i') \tag{5}$$

$$Subject\ to \begin{cases} y_i - w^T.x - b \le \xi_i + \varepsilon \\ w^T.x + b - y_i \le \xi_i' + \varepsilon \\ \xi_i, \xi_i', x_i \ge 0 \end{cases}$$

In this equation, the parameters of ξ_i and ξ_i' represent the slack variables. Such variables apply constraints over the function. In fact, a function is fitted to the imported data so that no training error is miniaturized, and more than this, such sophisticated functions are penalized. As it is evident, the above equation is composed of two terms: the first one indicates the Vapnik-Chervonenkis confidence interval. The second term shows the empirical risk. Those terms restrict the higher boundary of the generalization error instead of the training error. In other words, the SVR approach produces an equilibrium between those two terms. This equilibrium gives rise to a modified generalization performance which is more appropriate in comparison to the ANN algorithms [43]. In addition, in the above relationship, *C* simultaneously guarantees the maximization of the ε and minimization of the error,ξ. Based on this equation, if an error is lower than the ε, it will not need a nonzero ξ_i or ξ_i', and also, it will not be incorporated into the objective function [22]. Applying the Lagrange multipliers of α and α', and adopting the constraints of $C > 0$, and $\varepsilon > 0$, the formula of the optimum hyperplane is acquired through the maximization of the underlying equation:

$$R_{reg}[f] = \frac{1}{2}||w||^2 + C.R^{z}_{emp}[f]$$
$$where \quad R^{z}_{emp}[f] = \frac{1}{m}\sum_{i=1}^{m} |y_i - f(x_i)|_z \tag{6}$$

$$Subject\ to\ 0 \le (\alpha_i - \alpha_i') \le C \tag{7}$$

For a more appropriate indication of the data in the nonlinear case, the data points are mapped through an alternative space [44]. Such space is commonly known as the feature space through the underlying change:

$$x_i.x_j \rightarrow \phi(x_i).\phi(x_j) \tag{8}$$

There is no need to know the functional form of the mapping, $\varphi(x_i)$. The reason is that $\varphi(x_i)$ is implicitly determined using a specific kernel function, $k(x_i,x_j) = \varphi(x_i).\varphi(x_j)$, or inner product in the Hilbert space. If an appropriate kernel function is selected, the data can be separated in the feature space. At the same time, the original input space is kept in the nonlinear form. In this research, the Gaussian kernel has been utilized. The corresponding mathematical relationship is presented in Table 1. In section (6.1), the details of this kernel have been elaborated. Therefore, the nonlinear regression estimation can be written as [9, 19, 22]

$$y_i = \sum_{i=1}^{N}\sum_{j=1}^{N}(\alpha_i - \alpha_i')\phi(x_i)^T\phi(x_j) + b = \sum_{i=1}^{N}\sum_{j=1}^{N}(\alpha_i - \alpha_i')K(x_i, x_j) + b \tag{9}$$

where the variable of *b* is calculated when the constraints of Equation (5) get $\xi_i = 0$ if $0 < \alpha_i < C$, and $\xi_i' = 0$ if $0 < \alpha_i' < C$.

Table 1. Kernel type used in this research [34].

Mathematical form	Kernel type
$K(x_i, x_j) = exp\left[\|x_i - x_j\|^2 / 2\sigma^2\right]$	Gaussian Kernel

The training process of the SVM models can be performed through several algorithms. To do this, the Sequential Minimal Optimization (SMO) is an appropriate option due to its vast benefits [45]. In fact, such an algorithm provides users with simplicity and high computation-efficiency. In addition, the SMO algorithm does not require to deploy the numerical quadratic programming optimization step. An SMO model possesses two principal approaches: one is the analytic approach which solves both Lagrange multipliers. The other one includes a heuristic approach in order to select the multipliers during the optimization step [46].

As the solution of the two Lagrange multipliers is conducted analytically, the requirement of the numerical quadratic programming optimization might be entirely met [46, 47]. Furthermore, this algorithm needs less computer capacity for matrix storage; such merit helps the users to solve the complex SVM training problems through a usual computer. In this research, the authors have used the SMO algorithm to optimize the SVM predictive model, and to predict the copper grades of the high-grade copper zones, in a reasonable running time. The SVM models was implemented with a Gaussian Radial Basis Function (RBF) kernel. The critical hyperparameters were optimized through rigorous testing: regularization parameters C: 2400, kernel parameters σ=0.015, and epsilon-tube ε= 0.00001.

2.5. BPNN technique and implementation

Artificial neural networks (ANNs) provide computational models to mimic the function of biological neural structures. Furthermore, the recurrent neural networks are considered as proficient approaches to conduct the nonlinear adaptive filtering [8, 46]. Such applications have

been utilized in a wide range of scientific issues [48]. Furthermore, the BPNN technique has a significant ability to generalize suitably on such issues. The BPNN approach is categorized among the supervised ML techniques, meaning that it is trained with a set of the available data [49]. While the training process is performed, the BPNN strives to fit the outputs with the reasonably close values. The training process commences with setting up a number of random weights. Afterward, the outputs are computed, and the corresponding estimation errors are calculated. Such error is adopted to update the weights, and it is continued till the ending criteria are satisfied.

The optimal BPNN architecture consisted of four layers: an input layer (4 neurons corresponding to select boreholes), two hidden layers (16 neurons each) with sigmoidal activation functions, and a single output neuron. The model was trained using the backpropagation algorithm with Bayesian regularization to prevent overfitting. Training convergence was set to terminate at either 1000 epochs or when the performance gradient fell below 1e-7.

2.6. Determination of the input dataset

As mentioned previously, the data (copper grades) related to twelve low- and medium-grade boreholes were used to estimate copper grades in the high-grade copper zone. The borehole CHF06 was situated in such a high-grade zone. Due to the porphyry nature of the deposit, no clear bond was observed between the copper grades in the borehole CHF06 and the rest. To solve this issue, the Genetic Algorithm-Artificial Neural Network (GA-ANN) and Principal Component Analysis (PCA) algorithms were deployed to choose the best input dataset for the SVM and BPPN models.

This approach was selected over simpler feature selection methods (e.g. correlation analysis) for a critical reason: the geological complexity of porphyry systems often results in highly non-linear relationships between different parts of the deposit. While a simple correlation might miss a meaningful but non-linear relationship, the hybrid GA-ANN is specifically designed to identify input variables that have a strong non-linear predictive power. PCA was integrated to enhance this process by reducing noise and multicollinearity in the input data, ensuring a more robust and generalizable model. This combined methodology is therefore essential for tackling the specific challenge of grade estimation in such a complex environment.

2.6.1. Genetic algorithm

In the 1970s, John Holland developed the genetic algorithms (GAs) which were based on the process of natural selection to solve the optimization and search problems. In a specific GA, a population of the candidate solutions (individuals) is selected, mutated, and evolved till the most appropriate solutions are achieved. In such an evolution process, every individual bears some features known as chromosomes. In fact, the evolution cycle is performed to keep the fittest individuals in the solution while the less competent ones are omitted from the irritation process. To do this, firstly a population composed of a random set of the generated individuals is selected, and then, it is evolved through the irritation processes. In each irritation, the new set of the individuals, known as the generation, undergoes the recombination and mutation processes. Omitting the incompetent individuals in each irritation, the ultimate generation will include the most fitted individuals. This process continues until the ultimate generation reaches the maximum fitness degree.

The GA-ANN algorithms perform the optimization process by evaluating the individuals' features encoded into the chromosomes. During the irritations, the chromosomes are altered, and mutated. The solutions are in the form of binary strings. Every GA-ANN algorithm has three biologically fundamental operators. The first one is called the selection operator; it chooses the more fit individuals through the irritations. This operation is known as the selection process. The second and third operators are the crossover and mutation, respectively [50]. Both of them perform the task of creation of new populations. The crossover operator works to vary the information amongst the individuals. On the other side, the mutation operator checks the desirable diversity [51]. Figure 5 indicates a schematic diagram used for GA-ANN and AI applications. In the current research, based on the mechanism performed by the GA-ANN algorithm, the best input dataset of the copper grades was determined through the subsequent procedure:

1) *Coding process*: Every chromosome has an equal number of genes and extracted features in its structure. In fact, all genes are coded using a binary number, i.e. 1 or 0, and locus associated with an input variable for the prediction process. When the binary number is equal to 1, the relevant feature is incorporated in the combination task. Having said this, if the binary number is equal to 0, the pertinent feature will not be incorporated in the combination task.

2) *Initial population*: Customarily, to generate the initial population, random sampling from the available input data combinations within the main dataset was conducted. A noteworthy point is that the population size has a determining impact on the computation-efficiency of the GA-ANN model as well as the accuracy of the results (grade estimations).

3) *Evaluation of the fitness function*: Fitness function is the seminal part of every GA-ANN algorithm. It assesses the estimation performance of the individual chromosomes (here, the coring specimens) utilized in the combination process. AI algorithms can compute and assess the fitness function.

4) *Choosing the most suitable structure of the GA algorithm*: As already mentioned, every GA-ANN algorithm applies three fundamental operators to solve the problem. The selection operator enhances the population through maintaining the more fit individuals, and omitting the less fit ones. The crossover operator contributes to modifying some genes of the individuals, thereby turning them to new, competent individuals. This act leads to remarkable enhancement of the GA's search proficiency. Furthermore, the mutation operator renders the binary codes of the genes reverse to save the population's diversity. Therefore, the frequency of the mutation and crossover of individuals is directly associated with their corresponding probabilities. Based on the repeated genetic operation, the most appropriate input data combinations related to the least fineness error are chosen for the prediction process. Numerous investigators have mitigated the necessity for the utilization of Genetic algorithm in optimization of the artificial neural networks [53, 9]. This is due to the capability of the GA-ANNs in solving the complex problems in which finding the most suitable input data and the best ANN's structure are difficult tasks. To generate the structure and weights of the artificial neural networks, some researchers suggested a calculation-efficient technique deploying the genetic algorithm [54, 55]. In the present paper, the GA-ANN together with the SVM and BPNN approaches are adopted to choose the best structure and input data for estimation of the high-grade copper zones in the Chah Firuzeh porphyry mine.

2.6.2. PCA Technique

This technique was initially introduced by [56], and was extended later by [57]. PCA is one of the most useful applications of linear algebra which contributes to solving the different neural networks problems. The wide applicability of PCA is due to its simplicity in extraction of the appropriate data from a complex dataset. In fact, it uses an orthogonal linear transformation capable of moving the data from the initial coordinate system to another one. This task is done so that the biggest variance through a number of scalar projections of the data puts on the first coordinate (known as the first principal component). Similarly, for the second, third, and subsequent biggest variance, this process is repeated. PCA has two main applications: dimensionality reduction, and finding the structural connections between the different variables. The dimensionality reduction means to reduce the size of a high-dimensional dataset to a low-dimensional one so that the main features of the larger dataset are transferred to the smaller one.

Such dimensional reduction is very helpful to slim down the size of the large datasets such as boreholes' grades. In this research, the PCA technique has been used to determine the most appropriate input dataset for the SVM and BPNN techniques.

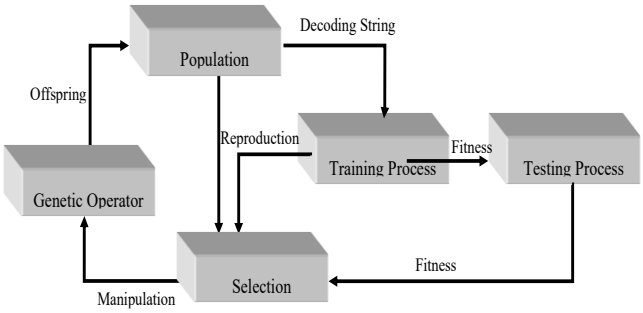

Figure 5. A Schematic flowchart of application of GA and AI techniques [52].

3. Results

3.1. Input selection

3.1.1. Selection of the input dataset by PCA

In order to reveal the hidden relationships between the copper grades in the aforesaid twelve boreholes and the borehole CHF06, a correlation matrix of the involved boreholes was achieved through the PCA algorithm. Table 2 presents the correlation coefficients pertinent to the various copper grades in the twelve boreholes with themselves, and with the borehole CHF06. As it is underlined in the above table, the correlation coefficients between the twelve boreholes with the borehole CHF06 are relatively high for four cases including the CHF05, CHF21, CHF24, and CHF26. The corresponding correlation coefficients for the boreholes CHF05, CHF21, CHF24 and CHF26 have been calculated as -0.401, 0.505, -0.615 and 0.602, respectively. However, poor correlations are very abundant for the rest of boreholes. For instance, the boreholes CHF01, CHF02, CHF08, CHF09, CHF13, CHF20 and CHF25 show poor approximation correlation coefficients with the CHF06 as 0.23, -0.292, 0.091, 0.021, -0.179, -0.106, -0.102 and -0.236, respectively. Hence, it can be stated that except for those four boreholes, there are no remarkable relations between the copper grades in the rest of the low- and medium-grade boreholes, and the borehole CHF06. From these observations, it was deduced that utilization of the linear and nonlinear approaches for establishing close correlations between the twelve boreholes, and the borehole CHF06 seems noticeably complex.

3.1.2. Selection the input dataset by GA-ANN

To assign the finest structures to the networks, two different codes were constituted using the MATLAB program. The GA-ANN was applied in both codes to optimize the model parameters, and to choose the foremost training data. Both codes were capable of choosing the length of the chromosomes utilized in the implementation of the optimal search. Consequently, for every network, the relative parameters were adjusted by individual chromosomes produced during the generation of population. The genes in the GA algorithm encompassed the σ, C, and ε. On the other side, the genes in the BPNN algorithm comprised the momentum, and learning rate. Based on the previous results conducted by the different researchers, the values of uniform mutation and cross-over operators were chosen, respectively equal to 0.01 and 0.5. After assigning those values, the GA was commenced using a number of 100 randomly generated chromosomes.

For determination of the population size in the GA model, there exists no unanimous manner. The size of the population can dramatically affect the training process of the input data; the reason is that each chromosome's fitness value must be assessed in each generation. Normally, in GA problems, a value of 20 to 100 is assigned to the population size [18, 42]. Therefore, in the current research, a number of 50 chromosomes were assigned to the initial population.

After the aforesaid arrangements, the GA was commenced with the initial 50 chromosomes. In the first irritation, the GA performs the evolution process through the individuals (solutions) of the initial population. As a consequence, the more fitted individuals survive, and the less qualified ones are eliminated. The surviving individuals then participated in the evolution of the second generation. Meanwhile, genetic operators improve the features of the individuals to form a new set of better solutions. For instance, through the crossover operator, two chromosomes swap their components for generation of two newer chromosomes for acceleration of the finding task of the optimal solution.

Similarly, in the subsequent irritations, the GA assesses the fitness of the newly generated individuals, and transfers the fitter ones into the next generations. The selection and transformation of the individuals is conducted by the selection operator. The selection operator applied in this research was the roulette wheel method. Therefore, the chance of picking up a chromosome, and incorporating it in the mating pool has a direct relation with the fitness value. Consequently, the survival of the most fitted chromosomes is guaranteed through those steps. Such cycles terminate when the GA reaches a satisfactory individual (solution), or particular criteria are satisfied. After fixing those key characteristics, in this research, the pertinent values of the input data for estimating the copper grades in the high-grade zone was determined by the GA-ANN algorithm. The values of the best fitness along with the mean fitness of the GA-ANN technique applied in the current research have been shown in Table 3.

After the analysis was performed, the GA-ANN algorithm delivered the relatively same results as the PCA algorithm. Figure 6 illustrates the chosen input data (i.e. the most suitable individuals) during the training process of the GA-ANN algorithm. As the figure shows, the best input parameters were selected as the boreholes CHF05, CHF21, CHF24, and CHF26. Hence, it can be said that the GA-ANN performs in a similar way with the PCA algorithm. From this finding it was inferred that such these four boreholes compose the best input dataset required to acquire the optimum fitness.

Table 2. Correlation matrix of copper concentration for twelve boreholes with borehole 6 in the Chah Firuzeh porphyry copper deposit.

	CHF01	CHF 02	CHF 05	CHF 06	CHF 08	CHF 09	CHF 13	CHF 20	CHF 21	CHF 22	CHF 24	CHF 25	CHF 26
CHF01	1.000												
CHF 02	-0.022	1.000											
CHF 05	0.072	-0.174	1.000										
CHF 06	0.230	-0.292	-0.401	1.000									
CHF 08	0.135	-0.035	0.078	0.091	1.000								
CHF 09	0.247	-0.316	-0.206	0.021	0.064	1.000							
CHF 13	-0.010	0.492	-0.296	-0.179	0.019	-0.210	1.000						
CHF 20	-0.177	-0.152	0.235	-0.106	-0.041	-0.172	-0.166	1.000					
CHF 21	-0.147	0.352	-0.281	0.505	0.110	-0.055	0.336	-0.158	1.000				
CHF 22	-0.214	0.027	0.232	-0.102	0.019	-0.242	0.187	0.187	-0.171	1.000			
CHF 24	-0.133	-0.204	0.257	-0.615	-0.053	-0.030	-0.229	0.527	-0.200	0.016	1.000		
CHF 25	0.100	0.403	-0.163	-0.236	-0.006	-0.193	0.340	-0.166	0.062	0.032	-0.211	1.000	
CHF 26	-0.069	-0.043	0.041	0.602	0.041	0.115	0.106	0.139	0.233	-0.054	0.092	-0.185	1.000

Table 3. Parameters of the GA-ANN algorithm to select the most appropriate input data of the different boreholes.

Method	Best fitness	Mean Fitness
GA-ANN	0.0128512	0.0201593

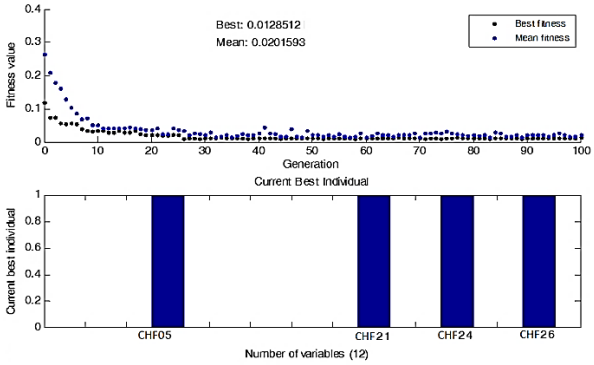

Figure 6. Selection of the most appropriate input data from the different boreholes by GA-ANN.

3.1. SVM and BPNN model performance

To increase the accuracy of the results predicted by the SVM technique, an optimum Kernel along with the other required parameters must be chosen properly. Numerous researchers have investigated the influence of the different, available kernel functions on the precision of the predicted results [9, 19, 46, 58]. Based on those investigations, the Gaussian kernel delivers reliable predictions due to its simplicity and computation-efficiency. The pertinent mathematical formula is expressed as:

$$K(x_i, x_j) = e^{-\|x_i - x_j\|^2 / 2\sigma^2} \quad (15)$$

In this equation, σ indicates a constant parameter controlling the amplitude of the Gaussian function or the generalization capability of the SVM model. Apart from the , the regularization parameter of C together with the insensitive parameter of ε should be optimally chosen. Generally, these three parameters have a highly influential impact on the predicted results

For instance, with regard to the regularization parameter of C, if it is selected very small or very large, the precision of the fitness function in the training process declines remarkably. Consequently, this pitfall will bring about notable calculation errors. Concerning the insensitive parameter of ε, if it is not properly selected, the training set will meet the boundary conditions, thereby rendering the network unstable during the testing phase. Furthermore, the BPNN predictive model possesses variables such as the momentum, and learning rates which must be chosen before the training phase of the network.

In this research, the ratio of training data to the testing data was selected as 70% to 30%, respectively. After performing the SVM algorithm, the optimum values of , , and C were computed as 0.015, 0.00001, and 2400, respectively. Moreover, for the BPNN model, the optimum networks encompassed four layers (Figure 7); the first one was an input layer comprising a number of four neurons (i.e. boreholes CHF05, CHF21, CHF24 and CHF26); the second and third ones were two hidden layers of sigmoidal function containing 16 neural, and the fourth one was the output layer consisting of only one neuron.

Figure 8 demonstrates the performance of the SVM model in prediction of the high-grade copper concentration in the borehole CHF06. Note that Cu% is the symbol of the copper grade. As can be seen, the coefficient of correlation has been obtained as 0.98, implying a high accuracy of the predicted (estimated) copper grades. The minimum and maximum copper grades in CHF06 borehole were predicted respectively as 0.05 and 1.05, which are very close to the real copper grades taken from the coring samples. In addition, as can be seen, the large proportion of the estimated and real copper grades falls within the range between 0.3% and 0.6%.

Similarly, Figure 9 illustrates the performance of the BPNN algorithm in prediction of the high-grade copper concentration in borehole CHF06. The coefficient of correlation was obtained as 0.72 which confirms the acceptable accuracy of the BPNN method in the estimation process. The predicted copper grades were in the same range with the real data. Similar to the SVM model, the majority of the predicted copper grades lied in the range of 0.3%-0.6%.

Similarly, Figure 9 illustrates the performance of the BPNN algorithm in prediction of the high-grade copper concentration in borehole CHF06.

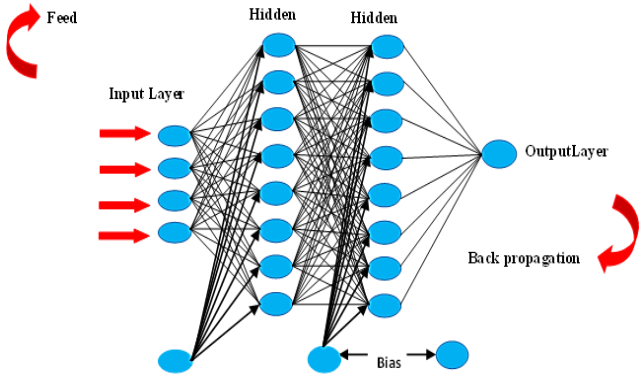

Figure 7. A schematic layout of the Block diagram of the optimum external BPNN structure.

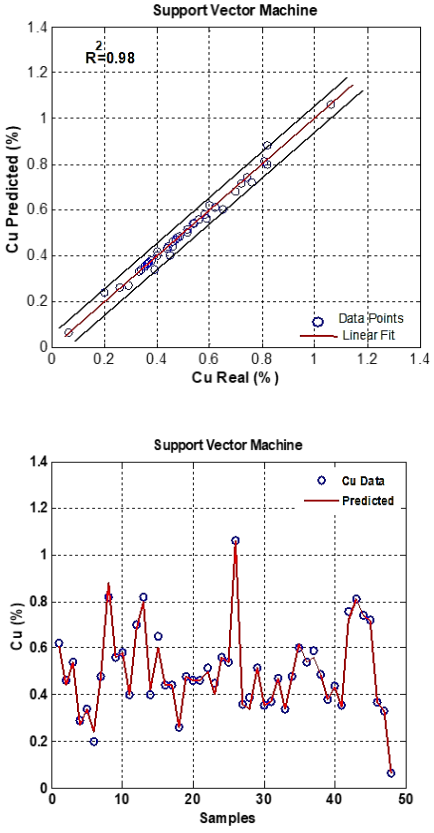

Figure 8. Correlation between the real (coring) and predicted (SVM) copper grades in borehole CHF06 (Up); Comparison between the real and predicted copper grades for different samples (Down).

The coefficient of correlation was obtained as 0.72 which confirms the acceptable accuracy of the BPNN method in the estimation process. The predicted copper grades were in the same range with the real data. Similar to the SVM model, the majority of the predicted copper grades lied in the range of 0.3%-0.6%.

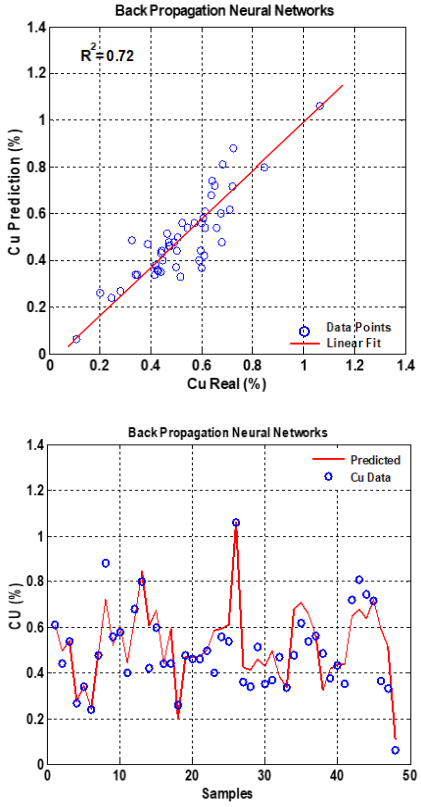

Figure 9. Correlation between the real (coring) and predicted (BPNN) copper grades in borehole CHF06 (Up); Comparison between the real and predicted copper grades for different samples (Down).

Based on the Figures 8 and 9, it can be expressed that the SVM model delivers more accurate estimations than the BPPN algorithm. Thus, it can be turned out the SVM approach is more reliable than the BPPN one. It is noteworthy that the superiority of the SVM model over the BPPN one may not always be true. In fact, further investigations and case studies related to the mineral grade estimation are required to support this hypothesis.

3.2. Effect of the input dataset

According to [58], this query may arise that whether the selected boreholes for the estimation process are the most appropriate or not. Another question is that if the proportion of the training data (or testing data) changes, does it affect the accuracy and efficiency of the networks or not?

To answer the first query, the effect of the input data on the copper grades predicted by the SVM model was probed. To do this, a number of eleven different datasets were deployed for the estimation task via the GA-ANN approach. Those datasets have been illustrated in Table 4. As an example, Dataset 1 encompasses input data (copper grades) from all twelve boreholes. In contrast, dataset 2 contained the entire input data of Dataset 1 without the borehole CHF01.

This procedure was repeated so that in each dataset one of the boreholes was excluded from the input data. Ultimately, the Dataset 11 consisted of only the input data relevant to the CHF24 and CHF26. After the GA-ANN algorithm was performed, the effect of input data on the accuracy of the predicted copper grades was revealed.

Table 4 shows the values of R^2 together with the *RMSE* of each network with different input dataset. As it is apparent, for both BPNN and SVM models, change in the input dataset shifts the R^2 and the *RMSE* of the training and testing steps. In this table, Dataset 9 has been underlined as the best dataset. Such Dataset includes the copper grades of the boreholes CHF05, CHF21, CHF24, and CHF26. As underlined, this dataset delivers the highest R^2 together with the lowest values of *RMSE* in comparison to other counterparts.

To answer the second query, firstly, the Dataset 9 was imported as the input data for the SVM and the BPNN models. Then, five tests were conducted with different ratios of the training data to the testing data, i.e. 90%/10%, 80%/20%, 70%/30%, 60%/40%, and 50%/50%, respectively. Table 5 depicts the values of the R^2 and *RMSE* for the corresponding networks.

Table 4. Variation of the accuracy of the SVM and BPNN algorithms with the different input datasets for prediction of the copper grades in borehole CHF06.

Model	Dataset	Input parameters	R^2 (Train)	R^2 (Test)	RMSE (Train)	RMSE (Test)
BPNN	Dataset 1	CHF 1, 2, 5, 8, 9, 13, 20, 21, 22, 24, 25 and 26	0.971	0.54	0.51	3.35
SVM			0.982	0.81	0.47	2.12
BPNN	Dataset 2	CHF 2, 5, 8, 9, 13, 20, 21, 22, 24, 25 and 26	0.972	0.56	0.51	3.21
SVM			0.982	0.83	0.46	2.03
BPNN	Dataset 3	CHF 5, 8, 9, 13, 20, 21, 22, 24, 25 and 26	0.973	0.57	0.50	3.18
SVM			0.983	0.85	0.46	1.91
BPNN	Dataset 4	CHF 5, 9, 13, 20, 21, 22, 24, 25 and 26	0.984	0.60	0.46	2.95
SVM			0.991	0.88	0.44	1.54
BPNN	Dataset 5	CHF 5, 13, 20, 21, 22, 24, 25 and 26	0.989	0.64	0.44	2.75
SVM			0.997	0.91	0.41	1.22
BPNN	Dataset 6	CHF 5, 20, 21, 22, 24, 25 and 26	0.991	0.66	0.44	2.59
SVM			0.998	0.92	0.44	1.12
BPNN	Dataset 7	CHF 5, 21, 22, 24, 25 and 26	0.992	0.68	0.44	2.27
SVM			0.999	0.95	0.43	0.96
BPNN	Dataset 8	CHF 5, 21, 24, 25 and 26	0.993	0.70	0.44	2.09
SVM			0.999	0.96	0.42	0.90
BPNN	Dataset 9	CHF 5, 21, 24 and 26	0.995	0.72	0.40	1.89
SVM			0.999	0.98	0.40	0.75
BPNN	Dataset 10	CHF 21, 24, and 26	0.990	0.67	0.46	2.35
SVM			0.995	0.96	0.44	0.91
BPNN	Dataset 11	CHF 24 and 26	0.988	0.65	0.49	2.65
SVM			0.993	0.94	0.46	0.99

Table 5. Variation of the accuracy of the SVM and BPNN algorithms with the different ratio of the training data to the testing data for prediction of the copper grades in borehole CHF06. The input data included the copper grades from the boreholes CHF05, CHF21, CHF24, and CHF26.

Model	Training/testing (%)	R^2 (Train)	R^2 (Test)	RMSE (Train)	RMSE (Test)
BPNN	90/10	0.999	0.68	0.44	2.59
SVM		0.999	0.95	0.42	0.92
BPNN	80/20	0.999	0.69	0.43	2.41
SVM		0.999	0.95	0.41	0.91
BPNN	70/30	0.999	0.72	0.40	1.89
SVM		0.999	0.98	0.39	0.75
BPNN	60/40	0.990	0.65	0.54	2.89
SVM		0.991	0.94	0.45	0.97
BPNN	50/50	0.974	0.55	0.68	3.07
SVM		0.982	0.91	0.53	1.04

According to this table, the change in the ratio of the training data to the testing data alters the accuracy of the results. More importantly, three conspicuous conclusions can be highlighted: firstly, when the ratio is 70%/30%, both SVM and BPNN models reach the highest accuracy. In better words, the R^2 and *RMSE* have, respectively, the highest and the lowest values amongst all five cases.

Secondly, the 50%/50% ratio is the worst case since it has the minimum R^2 and maximum *RMSE*. And thirdly, in all five cases, the accuracy of the SVM model is better than the BPNN model. This finding implies a lower sensitivity of the SVM algorithm to the ratio of training data to testing data. Hence, it can be said that the SVM algorithm is more reliable than the BPNN approach for prediction of complex resource estimation problems.

4. Discussion

4.1. Interpretation of model performance and SVM superiority

The remarkable performance disparity between the SVM (R^2 = 0.98, RMSE = 0.75) and BPNN (R^2 = 0.72, RMSE = 1.89) models can be attributed to their fundamental algorithm differences. SVM's principle of structural risk minimization enables it to find an optimal hyperplane that maximizes the margin between different data classes, thereby enhancing generalization to unseen data.

This characteristic is particularly advantageous in porphyry copper deposits like Chah Firuzeh, where grade distribution is often erratic. SVM's inherent resistance to overfitting, even with limited high-grade training data from a single borehole (CHF06), allowed it to capture the underlying genetic relationship between low-medium grade zones and the high-grade core. In contrast, BPNN's reliance on empirical risk minimization makes it more susceptible to local minima and overfitting, especially when the feature space is complex and target class data is sparse. The consistency of SVM's performance across different training-testing ratios further underscores its robustness as a more reliable estimator for this specific geostatistical challenge.

4.2. Geological significance of input selection

The convergence of both GA-ANN and PCA algorithm on the same set of input boreholes-CHF05, CHF21, CHF24, and CHF26- reflects a deeper geological control rather than mere statistical coincidence. The strong positive correlations with CHF21 (0.505) and CHF26 (0.602) suggest these boreholes likely share the same mineralized potassic core or are connected through a common vein system with the high-grade CHF06 zone, indicating identical fluid sources and metal precipitation histories.

Conversely, the negative correlations with CHF05 (-0.401) and CHF24 (-0.615) provide crucial evidence of geochemical zonation. These boreholes are likely situated in peripheral alteration shells where copper may have been systematically remobilized ore depleted, creating an inverse geochemical relationship with the enriched core. This automated selection of geologically meaningful inputs validates our integrated workflow as a powerful tool for feature selection that aligns perfectly with geological intuition and porphyry deposit models.

4.3. Methodological comparison and innovation

While SVM and BPNN are established methods, our study introduces significant innovation through their integrated application to solve a specific, challenging scenario in mineral exploration: estimating high-grade zones using exclusively low-and medium-grade data. The synergistic combination of GA-ANN and PCA for robust input variable selection ensures that models are fed with the most geologically relevant information, addressing the common "garbage in, garbage out" dilemma in geoscience AL applications. Compared to recent deep learning approaches like LSTMs, our methodology is specifically optimized for represents a deliberate and context-aware balance between model complexity, data availability, and interpretability, making it particularly valuable for real-world exploration scenarios where data is often constrained.

4.4. Practical implications and future research directions

The practical implications of this research extend beyond academic modeling to direct industry applications. Mining companies facing limited high-grade data can employ this methodology as a cost-effective strategy for estimating mineral potential and de-risking exploration campaigns. For instance, virtual boreholes can be simulated in unexplored areas due to topographic constrains or environmental protections, enabling resource estimation without the time and expense of additional drilling.

Several limitations naturally point toward future research directions: 1) generalizability testing of this workflow on other porphyry deposits with multiple known high-grade zones is essential. 2) external validation with newly acquired drilling data from separate zones should be prioritized when available. 3) Multi-data integration incorporating mineralogical, multi-element geochemical, and geophysical data could further enhance model accuracy and geological insight. 4) Advanced deep learning exploration using Convolutional Neural Networks (CNNs) for true 3D spatial data analysis presents a promising avenue for next-generation resource estimation.

5. Conclusion

In this research, two different AI approaches including the SVM and BPPNN were applied to estimate the high grades of copper in the Chah Firuzeh copper deposit situated in Kerman Province, Iran. Among the thirteen exploratory boreholes drilled in the area, only one borehole (CHF06) had reached the high-grade copper zone. To select a suitable AI technique for the future resource estimation works in the project, the capability of the SVM and BPPNN in prediction of copper grades was evaluated.

The first step was the selection of the most suitable input dataset (low and medium copper grades) from the low- and medium-grade boreholes to reach the best fitness function in the SVM and BPNN analyses. Both GA-ANN and PCA algorithms detected that the copper grades of the boreholes CHF05, CHF21, CHF24, and CHF26 comprise the best input dataset. Thus, those copper grades were used as the input data in the subsequent grade estimation performed via the SVM and BPNN techniques.

According to the results, the SVM algorithm (R^2=0.98 and *RMSE (Test)* =0.75) delivers the most accurate estimation of the copper grades in the high-grade zone. On the other hand, the estimation performance of the BPNN model (R^2=0.72 and *RMSE (Test)* =1.89) was found to be relatively acceptable although its efficiency is less than the SVM algorithm.

To justify the significant capability of the SVM algorithm over the other two techniques, it can be said that the SVM is less sensitive to the noises and outliers in the input dataset. As in the porphyry metal deposits, the spatial distribution of the mineral grade is commonly inconsistent, and the SVM algorithm can be a suitable AI technique to solve resource estimation problems. Hence, it can be turned out that the SVM algorithm performs highly accurate estimations when the mineral distribution is uniform, e.g. iron massive deposits. It is recommended that, for resource estimation problems, the SVM algorithm is applied to acquire more reliable predictions, and to plan the financial perspective of the mining operations with low potential risks.

From the results, it is concluded that the SVM algorithm can be applied for resource estimation tasks, particularly in two problematic cases: the first case is when the mineral distribution in the deposit is inconsistent, e.g. the porphyry deposits. The second case is when a challenging natural barrier (mountain, valley, river, road, etc.) or an environmentally protected area lies in a part of the deposit. In this situation, an imaginary borehole can be assumed on a specific location in the area, and then its grades are estimated by the SVM algorithm. Through this, without drilling and spending huge amount of time and budget, a borehole can be simulated and added to the network of the initial exploratory boreholes. This is a very efficient application in terms of time and cost for mining companies.

References

[1]. Mostafaei, K. and Ramazi, H. Mineral Resource estimation using a combination of drilling and IP-Rs data using statistical and cokriging methods. Bulletin of the mineral research and exploration. 2019; 160: 177-195.

[2]. Yama, B.R., Lineberry, G.T. Artificial neural network application for a predictive task in mining. Mining Engineering. 1999; 51: 59 – 64.

[3]. Tahmasebi, P. and Hezarkhani, A. Application of adaptive neuro-fuzzy inference system for grade estimation; case study, Sarcheshmeh porphyry copper deposit, Kerman, Iran. Australian Journal of Basic and Applied Sciences. 2010; 4(3): 408-420.

[4]. Rumelhart, D.E., Hinton, G.E., Wiliams, R.J. Learning representations by back-propagating errors. Nature. 1986; 323: 533-536.

[5]. Fahlman, S.E. Faster-learning variations of back-propagation: An empirical study. In 1988 Connectionist Models Summer School. Morgan Kaufmann. 1998: 38-51.

[6]. Clarici, E., Owen, D., Durucan, S., Ravencroft, P. Recoverable reserve estimation using a neural network. In 24th International Symposium on the Application of Computers and Operations Research in the Minerals Industries (APCOM), Montreal, Quebec.1993: 145-152.

[7]. Hagan M.T., Menhaj, M. Training feed forward networks with the Marquardt algorithm. IEEE Trans, Neural Networks.1994; 5(6): 989-993.

[8]. Wilamowski, B.M., Cotton, N.J., Kaynak, O., Dundar, G. Computing gradient vector and Jacobian matrix in arbitrarily connected neural networks. IEEE Transaction on industrial Electronic 56(10), 3784-3790 (2008).

[9]. Maleki, Sh., Moradzadeh, A., Ghavami, R., and Sadeghzadeh, F. A Robust Methodology for Prediction of DT Wireline Log. Iranian Journal of Earth Sciences. 2013; 5, 33-40.

[10]. Mostafaei, K. and Ramazi, H. Investigating the applicability of induced polarization method in ore modelling and drilling optimization: a case study from Abassabad, Iran. Near Surface Geophysics.2019; 17:637-652.

[11]. Lin, N., Chen, Y., Liu, H., & Liu, H. A comparative study of machine learning models with hyperparameter optimization algorithm for mapping mineral prospectivity. Minerals. 2021; 11(2): 159.

[12]. Chen, G., Huang, N., Wu, G., Luo, L., Wang, D., & Cheng, Q. Mineral prospectivity mapping based on wavelet neural network and Monte Carlo simulations in the Nanling W-Sn metallogenic province. Ore Geology Reviews.2022; 143: 104765.

[13]. Chen, F., Tiwari, S., Mohammed, K. S., Huo, W., & Jamróz, P. Minerals resource rent responses to economic performance, greener energy, and environmental policy in China: Combination of ML and ANN outputs. Resources Policy.2023; 81, 103307.

[14]. Yousefi, M., Lindsay, M. D., & Kreuzer, O. Mitigating uncertainties in mineral exploration targeting: Majority voting and confidence index approaches in the context of an exploration information system (EIS). Ore Geology Reviews. 2024; 105930.

[15]. Wu, X., Zhou, Y. Reserve estimation using neural network techniques. Computers and Geosciences, 1993; 19: 567-575.

[16]. Kapageridis, I. Input space configuration effects in neural network-based grade estimation. Computers & Geosciences. 2005; 31: 704-717.

[17]. Burnett, C.C. Application of neural networks to mineral reserve estimation, Ph.D. Dissertation, Department of Mineral Resources Engineering, University of Nottingham, Nottingham, 254 p. 1995.

[18]. Badel, M., Angorani, S., Shariat Panahi, M. The application of median indicator kriging and neural network in modeling mixed population in an iron ore deposit. Computers and Geosciences. 2010; 37: 530-540.

[19]. Maleki, Sh., Moradzadeh, A., Riabi, R.G., Sadaghzadeh, F. Comparison of Several Different Methods of in situ stresses determination, International Journal of Rock Mechanics & Mining Sciences. 2014; 71: 395-404.

[20]. Kapageridis, I., Denby, B. Ore grade estimation with modular neural network Systems-a case study. Information Technology in the Mineral Industry. In G. N. Panagiotou and T. N. Michalakopoulos, eds., Information technologies in the minerals industry: A. A. Balkema Publishers, Rotterdam, p. 52 (1998).

[21]. Vapnik, V. The nature of statistical learning theory. Springer science & business media. 1999. DOI 10.1007/978-1-4757-3264-1.

[22]. Maleki, Sh., Moradzadeh, A., Riabi, R.G., Gholami, R., Sadaghzadeh, F. Prediction of shear wave velocity using empirical correlations and artificial intelligence methods. NRIAG Journal of Astronomy and Geophysics. 2014; 3:70-81.

[23]. Cristianini, N. Shawe-Taylor, J. An introduction to support vector machines and other kernel-based learning methods. Cambridge university press. 2000.

[24]. Zuo, R., & Carranza, E. J. M. Support vector machine: A tool for mapping mineral prospectivity. Computers & Geosciences.2011; 37(12): 1967-1975.

[25]. Zhang, N., Zhou, K., & Li, D. Back-propagation neural network and support vector machines for gold mineral prospectivity mapping in the Hatu region, Xinjiang, China. Earth Science Informatics.2018; 11: 553-566.

[26]. Xiong, Y., & Zuo, R. Recognizing multivariate geochemical anomalies for mineral exploration by combining deep learning and one-class support vector machine. Computers & geosciences.2020; 140: 104484.

[27]. Mostafaei, K., Maleki, S., Jodeiri Shokri, B., & Yousefi, M. Predicting gold grade by using support vector machine and neural network to generate an evidence layer for 3D prospectivity analysis. International Journal of Mining and Geo-Engineering.2023; 57(4): 435-444.

[28]. Zheng, C., Yuan, F., Luo, X., Li, X., Liu, P., Wen, M & Albanese, S. Mineral prospectivity mapping based on Support vector machine and Random Forest algorithm-A case study from Ashele copper-zinc deposit, Xinjiang, NW China. Ore Geology Reviews. 2023; 105567.

[29]. Bilal, A., Imran, A., Baig, T. I., Liu, X., Long, H., Alzahrani, A., & Shafiq, M. Improved Support Vector Machine based on CNN-SVD for vision-threatening diabetic retinopathy detection and classification. Plos one. 2024; 19(1): e0295951.

[30]. Olya, B. A. M., & Mohebian, R. E. Z. A. Q-factor estimation from vertical seismic profiling (vsp) with deep learning algorithm, cudnnlstm. Journal of Seismic Exploration, 2023; 32, 89-104.

[31]. Rajabi, A., Mahmoodi, P., Rastad, E., Niroomand, S., Peernajmodin, H., Akbari, Z., & Haghi, A. A review of fluid inclusion investigations on Cretaceous sediment-hosted Zn-Pb (±Ba±Fe±Ag±Cu) deposits in the Malayer-Esfahan metallogenic belt (MEMB). 2019; In Third Biennial Iranian National Fluid Inclusion conference.

[32]. Rajabi, A., Rastad, E., Mahmoodi, P., Niroomand S., Peernajmodin, H., Movahednia, M., Fadaei, M., Olya, B. A. M., Boveiri, M. Zinc-Lead (± Ba ± Fe ± Ag ± Cu) mineralization in Malayer-Esfahan metallogenic belt, 2019: The 7th National Conference on Geomorphology and Structural Geology of Iran.

[33]. Hezarkhani, A. A Fluid Inclusion Investigation on Chah-Firuzeh Porphyry Copper Deposit, Based on Drill Core No. 6, Ahar Copper Company, Internal report, p. 42; 2007.

[34]. Hezarkhani, A. Hydrothermal fluid geochemistry at the Chah-Firuzeh porphyry copper deposit, Iran: Evidence from fluid inclusions, Journal of Geochemical Exploration. 2009; 101: 254–264.

[35]. Scholkopf, B., Smola, A.J., Muller, K.R. Nonlinear component analysis as a kernel igenvalues problem, Neural Computed.1998; 10: 1299-1319.

[36]. Mostafaei, K., Maleki, S., Zamani M.A.M Knez, D. Risk management prediction of mining and industrial projects by support vector machine. Resources Policy. 2022; 78 .1-8.

[37]. Tran, Q.A., Li, X. and Duan, H. Efficient performance estimate for one-class support vector machine. Pattern Recognition Letters.2005; 26: 1174-1182.

[38]. Walczack, B., Massart, D.L. The radial basis functions-partial least squares approach as a flexible non-linear regression technique. Anal.Chimical Acta. 1996; 331: 177-185.

[39]. Al-Anazi, A.F., Gates, I.D. Support vector regression for porosity prediction in a heterogeneous reservoir: A comparative study. Computers and Geosciences.2010; 36: 1494-1503.

[40]. Keerthi, S.S., Lin, C.J. Asymptotic behaviors of support vector machines with Gaussian kernel. Neural Computation.2003; 15(7): 1667-1689.

[41]. Schölkopf, B., Smola, A.J. and Bach, F. Learning with kernels: support vector machines, regularization, optimization, and beyond. MIT press. London, England. 2002.

[42]. Li, Q., Licheng, J., Yingjuan, H. Adaptive simplification of solution for support vector machine, Pattern Recognition. 2007; 40: 972 -980.

[43]. Wu, C.H., Tzeng, G.H., Lin, R.H. A Novel hybrid genetic algorithm for kernel function and parameter optimization in support vector regression. Expert Systems with Applications.2009; 36: 4725-4735.

[44]. Wang, L. Support Vector Machines: Theory and Applications, Springer Science & Business Media. 2005.

[45]. Platt, J. Sequential minimal optimization: A fast algorithm for training support vector machines. 1998.

[46]. Maleki Sh., Ramazi H.R., Moradi S. Estimation of Iron Concentration by Using a Support Vector Machine and an Artificial Neural Network - the Case Study of the Choghart Deposit southeast of Yazd, Yazd, Iran. Geopersia.2014; 4(2): 201-212.

[47]. Khanlari, G.R., Heidari, M., Momeni, A.A., Abdilor Y. Prediction of shear strength parameters of soils using artificial neural networks and multivariate regression methods. Engineering Geology.2012; 131-132:11-18.

[48]. Plett, G.L. Adaptive inverse control of linear and nonlinear systems using dynamic neural networks. IEEE Transactions Neural Network. 2003; 14 (2): 360-376.

[49]. Jin, L., Gupta, M.M. Stable dynamic back propagation learning in recurrent neural networks. IEEE Transactions on Neural Network.1999; 10(6): 1321-1334.

[50]. Reformat, M. Application of Genetic Algorithms in Control Design for Advanced Static VAR Compensator at ac/dc Interconnection. University of Manitoba Press, Canada. 1997.

[51]. Bandyopadhyay, S., Pal, S.K. Classification and learning using genetic algorithms: applications in bioinformatics and web intelligence. Springer Berlin, Heidelberg New York. 2007.

[52]. Saemi M., Ahmadi M., Yazdian Varjani A. Design of neural networks using genetic algorithm for the permeability estimation of the reservoir, Journal of Petroleum Science and Engineering.2007; 59: 97-105.

[53]. Hegazy, T., Fazio, P., Moselhi, O. Developing practical Neural Network applications using Back-propagation. Microcornputers in Civil Engineehg, Blackwelf Publishers.1994; 9(2): 145-159.

[54]. Van-Rooij, A.J.F., Jain, L.C., Johnson, R.P. Neural Network Training Using Genetic Algorithms, World Scientific Publishing. Singapore. 1996.

[55]. Vonk, E., Jain, L.C., Johnson, R.P. Automatic Generation of Neural Network Architecture Using Evolutionary Computation. World Scientific Publishing Co. Pvt. Ltd, Singapore. 1997.

[56]. Pearson, K. LIII. On lines and planes of closest fit to systems of points in space. The London, Edinburgh, and Dublin philosophical magazine and journal of science.1901; 2(11): 559-572.

[57]. Hotelling, H. Analysis of a complex of statistical variables into principal components. Journal of Educational Psychology. 1993; 24: 417–441.

[58]. Gholami, R., Moradzadeh, A., Maleki, Sh., Saman, A., Hanach, J. Applications of artificial intelligence methods in prediction of permeability in hydrocarbon reservoirs, Journal of Petroleum Science and Engineering.2014; 122: 643-656.